

Cutting is All You Need: Execution of Large-Scale Quantum Neural Networks on Limited-Qubit Devices

Alberto Marchisio^{1,2}, Emman Sychiuco^{1,2}, Muhammad Kashif^{1,2}, and Muhammad Shafique^{1,2}

¹eBRAIN Lab, Division of Engineering, New York University Abu Dhabi (NYUAD), Abu Dhabi, UAE

²Center for Quantum and Topological Systems (CQTS), NYUAD Research Institute, NYUAD, Abu Dhabi, UAE
alberto.marchisio@nyu.edu, jes9843@nyu.edu, muhammadkashif@nyu.edu, muhammad.shafique@nyu.edu

Abstract—The rapid advancement in Quantum Computing (QC), particularly through Noisy-Intermediate Scale Quantum (NISQ) devices, has spurred significant interest in Quantum Machine Learning (QML) applications. Despite their potential, fully-quantum QML algorithms remain impractical due to the limitations of current NISQ devices. Hybrid quantum-classical neural networks (HQNNs) have emerged as a viable alternative, leveraging both quantum and classical computations to enhance machine learning capabilities. However, the constrained resources of NISQ devices, particularly the limited number of qubits, pose significant challenges for executing large-scale quantum circuits.

This work addresses these current challenges by proposing a novel and practical methodology for quantum circuit cutting of HQNNs, allowing large quantum circuits to be executed on limited-qubit NISQ devices. Our approach not only preserves the accuracy of the original circuits but also supports the training of quantum parameters across all subcircuits, which is crucial for the learning process in HQNNs. We propose a cutting methodology for HQNNs that employs a greedy algorithm for identifying efficient cutting points, and the implementation of trainable subcircuits, all designed to maximize the utility of NISQ devices in HQNNs. The findings suggest that quantum circuit cutting is a promising technique for advancing QML on current quantum hardware, since the cut circuit achieves comparable accuracy and much lower qubit requirements than the original circuit.

I. INTRODUCTION

Recent advances in Quantum Computing (QC), particularly with Noisy-Intermediate Scale Quantum (NISQ) devices, have shown groundbreaking progress and demonstrated quantum advantages in various fields [1]–[6]. However, due to the limitations of NISQ devices, standalone fully-quantum algorithms remain impractical. Hybrid Quantum-Classical Neural Networks (HQNNs) have emerged as an effective alternative, combining classical and quantum layers for machine learning applications [7]–[10]. HQNNs are robust against errors in NISQ devices [11], [12] and employ quantum circuits that interface between classical and quantum computations [13]. Angle embedding and amplitude embedding are commonly used to map classical data into quantum states [14], [15]. The angle embedding method consists of rotating each classical feature by a certain angle based on its magnitude, while the amplitude embedding encodes classical data into the amplitudes of a quantum state. The angle embedding, due to its 1-to-1 representation with the number of features into qubit states, is known for its high precision. On the other hand, using the amplitude encoding, n qubits are sufficient to encode 2^n features [14]. Hence, it can encode the information in a compact form.

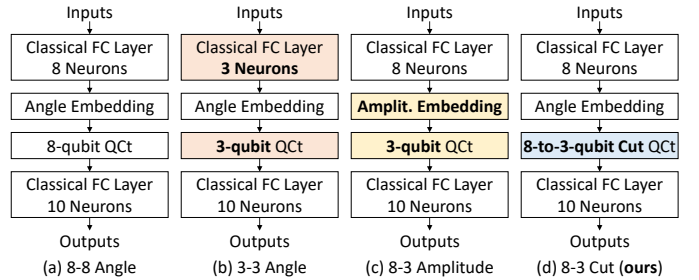


Fig. 1. Variants of the HQNN for this experiment. (a) Original HQNN, with an 8-neuron FC layer, angle embedding, 8-qubit quantum circuit (QcT), and 4-neuron FC layer. (b) Modified HQNN with reduced features, which has a 3-neuron FC layer and 3-qubit QcT. (c) Modified HQNN with amplitude embedding and 3-qubit QcT. (d) Modified HQNN with 8-to-3-qubit cut QcT.

A. Target Research Problem and Associated Challenges

The limited number of qubits and noisy nature of NISQ devices pose challenges in scaling quantum circuits [16]. Large-scale quantum circuits often suffer from noise, Barren plateaus [17], and computational overhead. The most prominent solutions for mitigating the noise in quantum circuits, namely quantum error correction and mitigation, further increase the demand for many-qubit circuits, since they introduce redundancies in quantum systems to reduce/eliminate the noise [18], [19].

Hence, there is a dire need to execute large-scale quantum circuits onto limited-qubit NISQ devices. Even the classical simulation of quantum circuits becomes extremely computationally and memory-intensive as well as requires very long execution times when simulating large-scale quantum systems. In this regard, Quantum circuit cutting [20] is a promising technique that partitions large circuits into smaller subcircuits, making it feasible to execute them on limited-qubit devices. However, existing quantum circuit cutting techniques [21]–[34] do not support gradient-based training for HQNNs¹. *Our work introduces a methodology that supports quantum circuit cutting while maintaining the backward propagation of gradients across subcircuits.*

B. Motivational Analysis

As a motivational case study, we analyze the training process of four different variants of HQNN models. We assume that

¹The current implementation of the automatic differentiation of quantum circuits [13] supports the conversion of a single quantum node (QNode) into Torch/Keras layer, but the cut circuit cannot be mapped onto a single QNode because it requires multiple nodes.

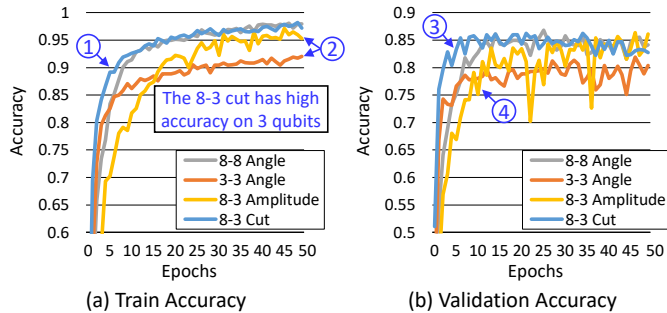


Fig. 2. (a) Training and (b) validation accuracy for different variants of the HQNN architecture on the Digits dataset.

the HQNN model in Figure 1a has the best architecture for the given application, which in this analysis is the classification on the Digits dataset [35]. This architecture is composed of a set of classical layers and quantum layers. A classical fully-connected (FC) layer with 8 neurons is followed by an 8-qubit quantum circuit and a classical FC layer with 10 neurons. The 8 classical features at the output of the first classical FC layer are encoded into quantum states with angle embedding. The final quantum states are then measured, and their values are used as input features of the following classical FC layer. The implementation, training, and hyperparameter details are discussed in Section IV-A.

However, we assume that only a 3-qubit quantum device is available. In this regard, Figure 1b, c, and d present three possible alternatives² to implement a modified version of the original circuit in a 3-qubit device. The 3-3 Angle architecture (version b) reduces the size of the first classical FC layer to 3 and maintains angle embedding to encode the three features into 3-qubit states. The 8-3 Amplitude architecture (version c) employs amplitude embedding to encode the 8 classical features into 3 quantum states in the 3-qubit device. The 8-3 Cut architecture (version d) employs the quantum circuit cutting technique to implement the 8-qubit circuit into multiple 3-qubit subcircuits in the 3-qubit quantum device.

The results of training and validation accuracy shown in Figure 2 highlight that the 8-3 Cut architecture provides the best solution in terms of accuracy compared to 3-3 Angle and 8-3 Amplitude. As indicated by labels ① and ③, the 8-3 Cut HQNN learns faster than the original 8-8 Angle HQNN in the first few training epochs. On the other hand, both 3-3 Angle and 8-3 Amplitude architectures do not reach the same level of accuracy of the original 8-8 Angle HQNN (see label ②). The lower accuracy of the 3-3 Angle HQNN is due to an information loss because only 3 features are propagated after the first FC layer, instead of 8. The 8-3 Amplitude HQNN has lower accuracy than the original 8-8 Angle and 8-3 Cut because of the different type of embedding used to encode the data. Moreover, as highlighted by label ④, the 8-3 Amplitude HQNN requires a larger number of epochs than other architectures to reach high validation accuracy.

²These three solutions do not form an exhaustive list of possibilities, but they provide a variety of solutions to solve the problem.

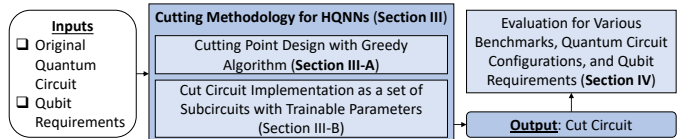


Fig. 3. Overview of the novel contributions in this work.

This simple yet insightful analysis demonstrates that *the approach with quantum circuit cutting has the potential to execute quantum circuits on limited-qubit devices with minimal changes to the rest of the HQNN architecture, maintaining similar accuracy levels compared to the original circuit.*

C. Novel Contributions

To solve the above-discussed challenges, we make the following novel contributions (see Figure 3):

- We propose a methodology for cutting HQNNs into multiple subcircuits, to enable their full execution on limited-qubit devices. (**Section III**)
- We design a greedy algorithm to automatically identify the cutting points in a given quantum circuit under a given qubit constraint for the underlying quantum device. (**Section III-A**)
- We implement the cut circuit as a set of subcircuits in a way that each node can be trained during the HQNN learning process. (**Section III-B**)
- We evaluate our methodology on various benchmarks and configurations of quantum circuits and qubit requirements. The experimental results demonstrate that the cut circuits achieve comparable accuracy to the original circuit with a small computation overhead, thereby enabling the execution of more complex circuits on limited-qubit devices. (**Section IV**)

II. BACKGROUND AND RELATED WORK

A. Hybrid Quantum-Classical Neural Networks

HQNNs are hybrid systems that combine classical and quantum computational elements, making them well-suited for NISQ devices [36]–[38]. In an HQNN, classical and quantum layers are integrated, typically in a sequential manner, allowing for a synergistic use of both types of computational resources [39]. Classical layers handle preprocessing, feature extraction, and output, while quantum layers perform complex operations like quantum feature mapping and entanglement. Similarly to the weights of the classical layers, the gates of the parameterized quantum circuits (PQCs) contain trainable parameters [40].

Classical data is transitioned into quantum layers by encoding it into quantum states through techniques such as angle embedding, which maps features to qubit rotations, or amplitude embedding, which compresses data into the quantum state’s amplitudes [14]. The quantum layers then process this data, leveraging high-dimensional feature spaces to analyze complex patterns. After quantum operations, the results are measured and fed back to the classical layers for further processing or decision-making [41]. The hybrid structure of HQNNs takes advantage of quantum computing’s strengths, such as parallelism and entanglement, while the classical layers mitigate the limitations of current quantum hardware [42]. This design

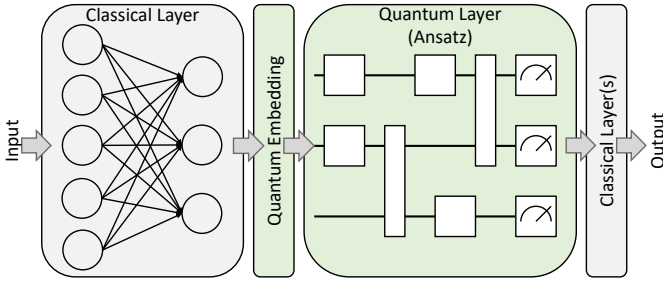


Fig. 4. Example of HQNN architecture, where a quantum layer is interleaved between classical layers.

enhances robustness against noise and errors and allows for greater scalability, making HQNNs a promising approach for advancing quantum machine learning, especially when fully-quantum networks are not yet feasible [36].

Figure 4 illustrates an example of an HQNN, where the input is processed through a classical layer, followed by the quantum embedding to encode the classical features into quantum states. After that, the quantum circuit (Ansatz) contains a set of gates that modify the state of the qubits, and the measurement operations read the values to be passed to the following classical layers. Finally, a set of one or more classical layers generates the output predictions. The outputs of the HQNNs are plugged into a loss function to train the parameters through classical backpropagation [43].

B. Quantum Circuit Cutting

Quantum circuit cutting has emerged as a solution to execute large circuits on small devices by breaking quantum wires using a measurement operation to save the values classically and reconstructing them across subcircuits by re-encoding the values into quantum states [20]. Figure 5 shows an example of this mechanism for a 5-qubit circuit implemented on 3-qubits.

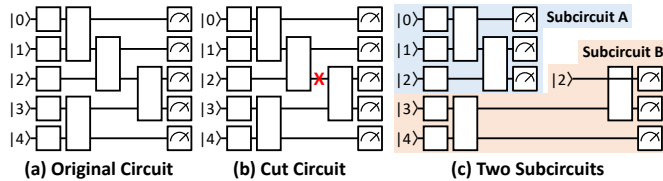


Fig. 5. Example of cutting a 5-qubit circuit to fit in a 3-qubit device. (a) Original circuit. (b) Cut circuit, where the cut is represented by a red cross. (c) Representation of the cut circuit as two 3-qubit subcircuits.

In recent years, several variants and optimizations of the quantum circuit cutting method have been proposed in the literature [21]–[34]. Moreover, quantum circuit cutting has been used for error mitigation [44]–[46].

However, these works are applied to quantum algorithms but not to QML and HQNNs. This is a major limitation because the current PennyLane implementations that convert quantum circuits to Keras layers³ or Torch layers⁴ require as input a single QNode. This is a fundamental step in HQNNs that allows to have trainable parameters in the quantum circuit. Since the cut

circuit cannot be implemented on a single QNode but requires multiple QNodes (one for each subcircuit), the quantum circuit cutting in its form cannot be adopted in HQNNs. To overcome this issue, our framework builds a QNode for each subcircuit and converts each QNode to a trainable Keras layer.

On the other hand, the works in [47], [48] are applied to QML but they only focus on quantum circuit partitioning. Similarly, the works in [49], [50] describe methods to execute HQNNs on distributed systems. However, the scope of our work is to provide a platform for employing quantum circuit cutting on HQNNs.

III. HQNN QUANTUM CIRCUIT CUTTING METHODOLOGY

Our methodology, depicted in Figure 6, starts with the original n -qubit quantum circuit and targets an m -qubit quantum device. The key steps involve designing optimal cutting points, generating subcircuits, and ensuring trainable parameters across the entire HQNN.

A. Cutting Points Design

The *Cutting Points Design Algorithm*, detailed in Algorithm 1, aims to identify optimal cutting points within a quantum circuit, enabling its execution on devices with a lower number of qubits than the original circuit. The algorithm starts by sorting the quantum gates based on their priority, determined by data dependencies within the circuit. Initially, the set of gates is divided into two groups: *UnmappedGates*, which contains all the gates to be processed, and *MappedGates*, which will store gates that have been successfully assigned to subcircuits.

The algorithm iterates by selecting n wires at a time, forming a subcircuit based on the device’s qubit limit. For each gate in the sorted list, the algorithm checks whether it can be implemented in the selected n -qubit subcircuit, while ensuring all its dependencies are satisfied. If all dependencies are available, the gate is moved from *UnmappedGates* to *MappedGates*. However, if a gate can be executed on the n -qubit subcircuit but has unresolved dependencies, the algorithm places a cut before this gate and proceeds to avoid mapping subsequent gates on the same wire within the current subcircuit. This ensures the circuit remains properly segmented based on qubit availability. The process repeats until all gates are successfully mapped, yielding a series of cut subcircuits, each capable of execution on a n -qubit device.

B. Cut Circuit Implementation

Our implementation of the cut circuit demonstrates the process of cutting the quantum circuit and integrating its subcircuits in the correspondent HQNN, having defined the cut placements within the original circuit. Subcircuits are generated by replacing cuts with measurement operations and re-encoding quantum states (using angle embedding). An example of subcircuit generation, based on the cuts in the original circuit, is shown in Figure 7.

After constructing the quantum circuit and applying the necessary cuts, the full HQNN model is assembled. The classical layers, are interwoven with the quantum subcircuits. Each subcircuit is described as an independent QNode and properly connected to each other to form the complete HQNN. In this

³https://pennylane.ai/qml/demos/tutorial_qnn_module_tf/

⁴https://pennylane.ai/qml/demos/tutorial_qnn_module_torch/

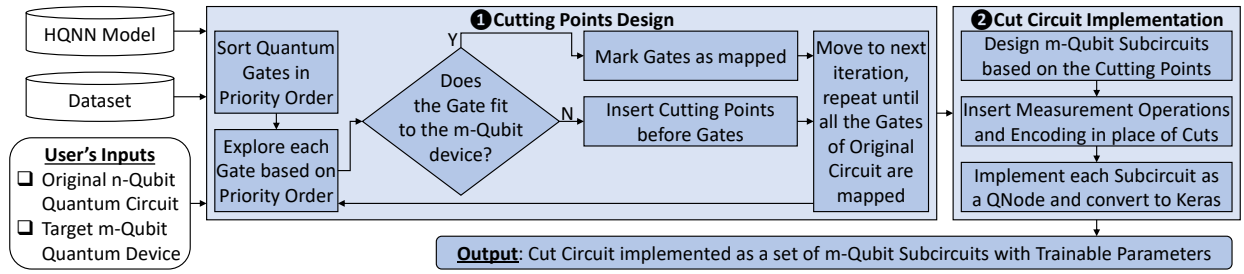


Fig. 6. Our methodology for cutting point design and implementation for HQNNs.

Algorithm 1: Cutting Points Design for Quantum Circuits

```

1 Procedure CuttingPointsDesign (Gates, n)
2   Sort Gates in Priority Order, from 1 to MaxGate;
   // priority based on the data
   // dependencies in the circuit
3   UnmappedGates ← Gates;
4   MappedGates ← ∅;
5   while UnmappedGates ≠ ∅ do
6     Select m wires based on priority; // This would
       form a m-qubit subcircuit
7     for UnmappedGates ∈ {1, ..., MaxGate} do
8       if UnmappedGatesi can be implemented in the
         n wires and all the dependencies are available
         then
9         Move UnmappedGatesi to
           MappedGates;
10        else if UnmappedGatesi can be implemented in
          the n wires but at least one dependency is not
          available then
11          Place a cut before UnmappedGatesi;
12          Do not consider the following gates on this
            wire as implementable in the n wires;
13        end
14    end
15 end

```

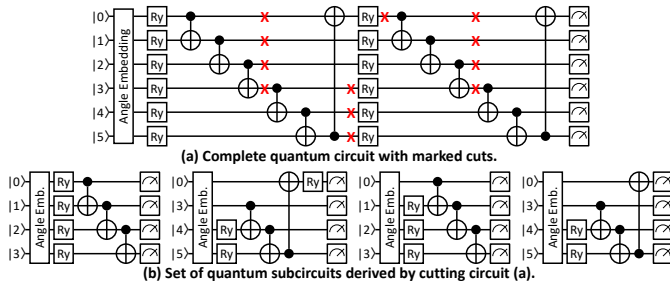


Fig. 7. Example of the generation of subcircuits in a 6-4 cut, given the original circuit and the cut placements.

way, all the subcircuits of the HQNN can be integrated into the network as quantum layers using PennyLane’s `KerasLayer`, which manages the parameterized quantum gates and their respective operations, using the traditional backpropagation mechanism.

During training, both the forward and backward passes are profiled to compute the number of floating-point operations (FLOPs), allowing for an analysis of the computational cost of the cut circuit implementation. Moreover, the training and validation accuracy values are measured and recorded for every training epoch.

IV. EVALUATION OF OUR CUTTING METHODOLOGY

A. Experimental Setup

The experiments are conducted on the Digits [35] and MNIST [51] datasets. Note that this is a typical settings for benchmarking HQNNs. The quantum circuits are implemented in PennyLane [13] with the Tensorflow Keras backend. The experiments run on a system equipped with an NVIDIA GeForce RTX 3060 GPU and AMD Ryzen 7 5800H CPU. The HQNN architecture consists of one classical fully-connected layer (where the number of neurons is equal to the number of qubits of the original quantum circuit), followed by a quantum layer with two repetitions of the basic entangling Ansatz, and another classical fully-connected layer with ten neurons (to match the number of classes of the datasets). The cut circuit experiments have been conducted sequentially on the same quantum system, which is reset and initialized iteratively for each subcircuit. All experiments are repeated five times to mitigate randomness, and the results show the average accuracy over these five runs. A detailed list of the experiment setup details and hyperparameters is visualized in Table I.

TABLE I
EXPERIMENT SETUP DETAILS

Item	Experiment Detail
Quantum Computing FrameWork	PennyLane
Back-End GPU Machine	NVIDIA GeForce RTX 3060
Deep Learning Interface	Tensorflow Keras API
Datasets	Digits & MNIST
Encoding	Angle Embedding
Optimizer	Adam
Epochs	50 & 200
Batch Size, Learning Rate	5, 0.01

B. Evaluation of our Cutting Methodology on the Digits Dataset

The results of cutting the circuits for the Digits dataset are shown in Figure 8. The results contain a set of n - m cut experiments, comparing the training and validation accuracy of the original n -qubit circuit with the cut circuit implemented on an m -qubit device. For different values of m and n , different observations can be derived. As indicated in labels ①, ②, and ③, for 4-2, 6-2, and 8-2 cuts there is quite a large gap between the training accuracy of the original circuit and the training accuracy of the cut circuit. A similar large gap can be observed for the validation accuracy. The reason for this discrepancy can be attributed to the fact that when the circuits are implemented on 2 qubits, the 2-qubit subcircuits

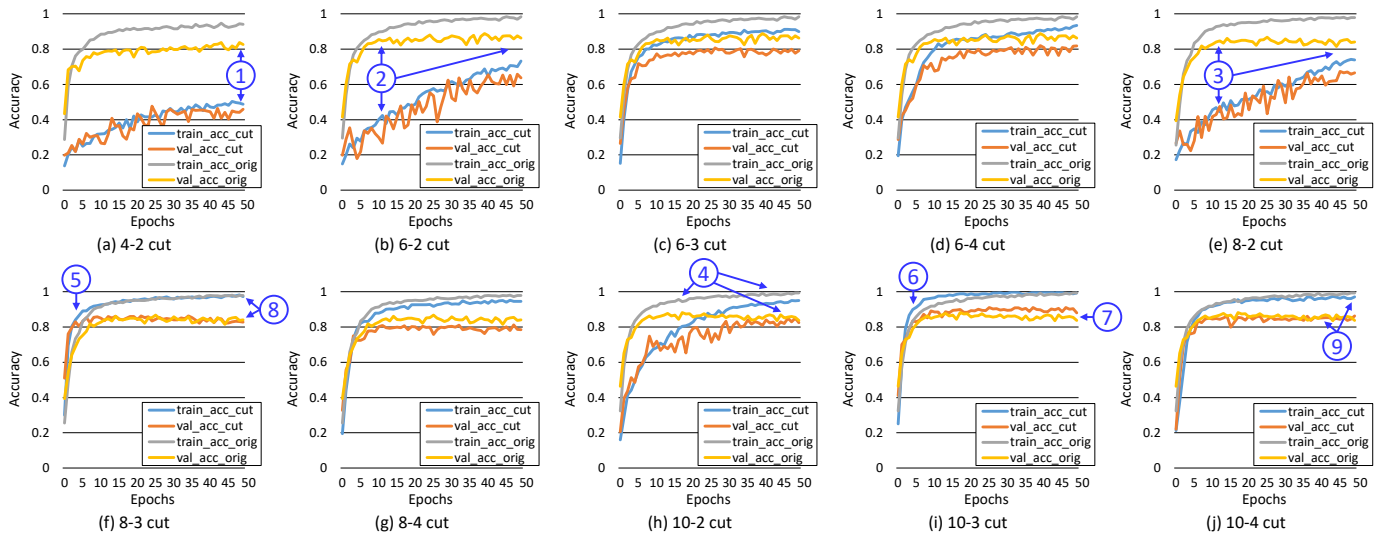


Fig. 8. Training and validation accuracy for the original and cut circuits with different numbers of qubits on the Digits dataset. Each plot shows the results for a n - m cut, with the n -qubit circuit implemented on an m -qubit device (using cutting) and compared with the original n -qubit circuit.

have low correlation and entanglement capabilities, which hinder the correct generalization of the problem.

However, for the 10-2 cut circuit, the results are slightly different (see label ④). While the training and validation accuracy gaps between the original circuit and the cut circuit are quite large after a few epochs, they shrink towards the end of the training epochs. This behavior suggested that the training process of the cut circuits implemented on a 2-qubit device might require more training epochs to reach higher accuracy. Hence, in Section IV-E, we analyze the behavior of these cut circuits when the HQNNs are trained for more epochs.

On the other hand, for devices that have more than 2 qubits, the training and validation accuracy of the cut circuits are comparable with the original circuit. As highlighted in labels ⑤ and ⑥ in Figure 8, for the 8-3 cut and 10-3 cut circuits, during the first few epochs, the training and validation accuracy of the cut circuits are higher than the original circuits, meaning that the cut circuits converge faster than the original circuit. Moreover, the validation accuracy of the cut circuit for the 10-3 cut even results slightly higher than the validation accuracy of the original circuits (see label ⑦). This can be attributed to a better generalization when the cuts are deployed in the circuit. For other cases (see labels ⑧ and ⑨), the training and validation accuracy curves for the original and cut circuits are overlapping, indicating that there is no significant functional difference between the two implementations.

C. Evaluation of our Cutting Methodology on the MNIST Dataset

Figure 9 shows the comparative results between the cut circuits and original circuits for the MNIST dataset. Overall, we can observe that the training and validation accuracy curves are similar for all the configurations. In some cases, for instance, for the 8-4 cut (see label ① in Figure 9), the training and validation accuracy of the cut circuit is slightly lower than that of the original circuit. In other cases, for the 6-4 cut and 10-3 cut circuits (see labels ② and ③). Moreover, we can observe that

for the first few epochs, the training and validation accuracies for the 8-3 cut circuit are higher than for the original circuit (see label ④).

Overall, the trends derived from the results conducted on both the Digits and MNIST datasets reveal good scalability and generalization for different benchmarks and workloads.

Note: we observe a certain level of overfitting in all the experiments, because the validation accuracy is significantly lower than the training accuracy. This phenomenon is well-known in neural networks and can be mitigated through techniques like dropout, regularization, and parameter adaptation [52]–[55]. However, tackling it is beyond the scope of this work, since we just demonstrate that our quantum circuit cutting approach can be applied to HQNNs.

D. Evaluation of the Impact of FLOPs Variations

To quantitatively measure the computational overhead when implementing the cuts, we measured the FLOPs required for both the forward and backward passes, for different configurations of original and cut circuits. Table II shows the results of our experiments on the Digits dataset. We can observe that, for all the configurations, cutting the circuits incurs an overhead in terms of FLOPs for the forward and backward passes. This overhead increases when reducing the number of qubits n of the target device. This behavior is justified by the fact that the computations in the cut circuit require additional measurement and encoding operations of the intermediate results, to store and retrieve the partial states when executing the computations across multiple subcircuits.

E. Ablation Study: Training Cut Circuits for More Epochs

Since the slope of the learning curves in some of the cut circuits is still high after 50 training epochs, we extended the training process to 200 epochs. Figure 10 shows the training and validation accuracy curves for the 4-2, 6-2, 8-2, and 10-2 cut circuits. We can observe that the accuracy plateau is reached after 120 epochs for the 6-2 and 8-2 circuits (see labels ① and ②

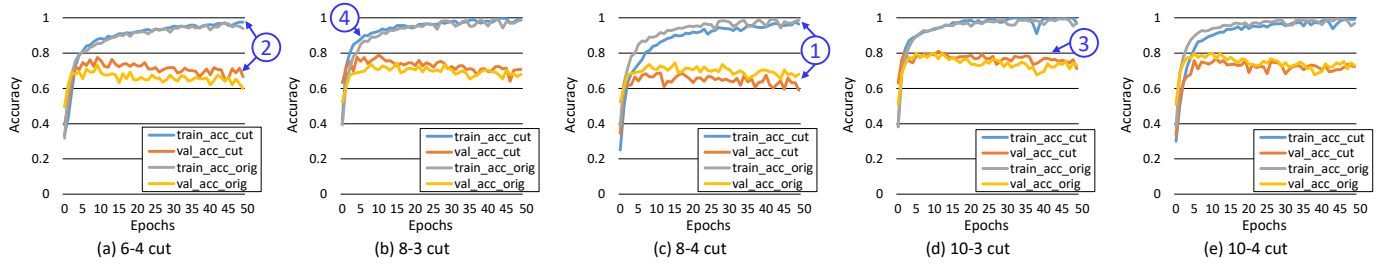


Fig. 9. Training and validation accuracy for the original and cut circuits with different numbers of qubits on the MNIST dataset.

TABLE II
RESULTS OF FORWARD (FW), BACKWARD (BW), AND TOTAL (TOT) NUMBER OF FLOPS FOR DIFFERENT VERSIONS OF THE ORIGINAL AND CUT CIRCUITS FOR THE DIGITS DATASET.

Circuit	4	4-2	6	6-2	6-3	6-4	8	8-2	8-3	8-4	10	10-2	10-3	10-4
FW FLOPs	48	96	72	192	132	108	96	320	208	160	120	480	300	240
BW FLOPs	230	306	404	554	494	478	602	866	754	716	852	1242	1062	1014
Tot FLOPs	278	402	476	746	626	586	698	1186	962	876	972	1722	1362	1254

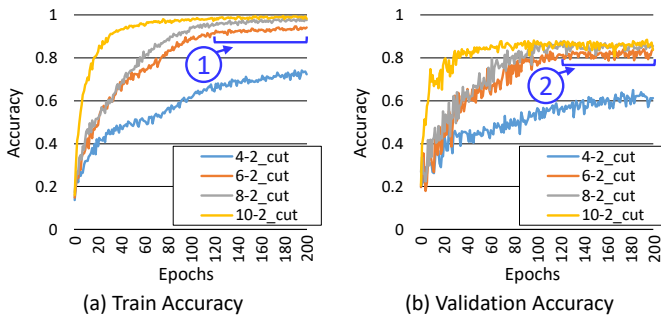


Fig. 10. (a) Training and (b) validation accuracy of 4-2, 6-2, 8-2, and 10-2 cut circuits, trained for 200 epochs on the Digits dataset.

in Figure 10). For higher qubits of the original circuit (i.e., for the 10-2 cut), the convergence appears after fewer epochs, while for lower qubits of the original circuits (i.e., for the 4-2 cut), more training epochs are required to obtain the convergence.

F. Discussion

The following key discussion points emerge from the experimental results:

- **Feasibility of the Method:** The experiments demonstrated the feasibility of training Hybrid Quantum-Classical Neural Networks (HQNNs) on devices with limited qubit capacity. The experimental findings indicate that the cut circuits perform similarly to the original circuits, establishing quantum circuit cutting as an effective strategy for training and implementing HQNNs on devices with only a few qubits. An exception to this trend is observed in circuits cut to 2 qubits, where a slower convergence rate and slight losses in training and validation accuracy were noted compared to the original circuit. However, when employing 3 or more qubits, the cut circuits closely mirror the performance of the original circuits, sometimes even surpassing them in certain cases.
- **Computational Overhead:** While there is a computational overhead associated with floating-point operations (FLOPs) in the cut circuits, the ability to execute the complete circuit on a reduced number of qubits significantly outweighs this cost. The reduced qubit requirement makes it possible to execute complex quantum circuits on hardware with limited resources,

a critical advantage in the current NISQ era.

- **Scalability:** This work serves as an initial proof-of-concept, demonstrating the practicality of training HQNNs on a limited number of qubits and proving the method’s scalability when applied to cut circuits. The experimental setup allows for relatively fast and practical comparisons between cut and uncut circuits, revealing a trend of adaptability and scalability toward larger-scale quantum circuits. Although the present experiments focus on a small number of qubits to illustrate the concept, the results suggest that the methodology is scalable to more complex circuits. Future work will focus on extending this approach to larger circuits, further exploring its potential.

V. CONCLUSION

This work addresses the pressing challenges of executing large-scale quantum circuits on NISQ devices by introducing a novel quantum circuit cutting methodology for HQNNs. This method allows for the implementation and training of HQNNs on devices with limited qubit capacity while preserving the accuracy of the original circuits. The proposed approach not only facilitates the execution of large quantum circuits on constrained hardware but also enables the learning process for quantum parameters in all subcircuits, a critical component for the effective training of HQNNs.

Our experiments have demonstrated that the cut circuits perform comparably to the original circuits in terms of accuracy, with minimal computational overhead, especially when using three or more qubits. The scalability and adaptability of this method were also confirmed, showing potential for deployment on larger circuits, thus addressing a significant limitation of current quantum computing hardware.

This work enables the implementation and training of HQNNs on quantum devices that have limited qubits, in such a way that large-scale quantum circuits in HQNNs are split into multiple subcircuits with a lower qubit requirement. The code and framework developed in this study will be made publicly available, ensuring reproducibility and fostering further advancements in the practical implementation of QML algorithms on NISQ devices.

ACKNOWLEDGMENT

This work was supported in part by the NYUAD Center for Quantum and Topological Systems (CQTS), funded by Tamkeen under the NYUAD Research Institute grant CG008.

REFERENCES

- [1] F. Arute *et al.*, “Quantum supremacy using a programmable superconducting processor,” *Nature*, vol. 574, p. 505–510, 2019.
- [2] I. F. Araujo *et al.*, “A divide-and-conquer algorithm for quantum state preparation,” *Scientific Reports*, 2020.
- [3] H.-Y. Huang *et al.*, “Quantum advantage in learning from experiments,” *Science*, 2022.
- [4] B. Pokharel and D. A. Lidar, “Demonstration of algorithmic quantum speedup,” *Physical Review Letters*, vol. 130, no. 21, 2023.
- [5] Y. Kim *et al.*, “Evidence for the utility of quantum computing before fault tolerance,” *Nature*, 2023.
- [6] A. Tudisco, D. Volpe, G. Ranieri, G. Curato, D. Ricossa, M. Graziano, and D. Corbelleto, “Evaluating the computational advantages of the variational quantum circuit model in financial fraud detection,” *IEEE Access*, vol. 12, pp. 102918–102940, 2024.
- [7] K. Zaman, A. Marchisio, M. A. Hanif, and M. Shafique, “A survey on quantum machine learning: Current trends, challenges, opportunities, and the road ahead,” *CoRR*, vol. abs/2310.10315, 2024.
- [8] S. Y.-C. Chen, T.-C. Wei, C. Zhang, H. Yu, and S. Yoo, “Quantum convolutional neural networks for high energy physics data analysis,” *Phys. Rev. Res.*, vol. 4, p. 013231, Mar 2022.
- [9] A. K. M. Masum *et al.*, “Hybrid quantum-classical machine learning for sentiment analysis,” in *ICMLA*, 2023.
- [10] R. L’Abbate, A. D’Onofrio, S. Stein, S. Y.-C. Chen, A. Li, P.-Y. Chen, J. Chen, and Y. Mao, “A quantum-classical collaborative training architecture based on quantum state fidelity,” *IEEE Transactions on Quantum Engineering*, vol. 5, pp. 1–14, 2024.
- [11] Z. Hu *et al.*, “On the design of quantum graph convolutional neural network in the nisq-era and beyond,” in *ICCD*, 2022.
- [12] M. Kashif, E. Sychiuco, and M. Shafique, “Investigating the effect of noise on the training performance of hybrid quantum neural networks,” *CoRR*, vol. abs/2402.08523, 2024.
- [13] V. Bergholm, J. A. Izaac, M. Schuld, C. Gogolin, and N. Killoran, “Pennylane: Automatic differentiation of hybrid quantum-classical computations,” *CoRR*, vol. abs/1811.04968, 2018.
- [14] M. Schuld and F. Petruccione, *Supervised Learning with Quantum Computers*. Springer Publishing Company, Incorporated, 2018.
- [15] M. Rath and H. Date, “Quantum data encoding: A comparative analysis of classical-to-quantum mapping techniques and their impact on machine learning accuracy,” *CoRR*, vol. abs/2311.10375, 2023.
- [16] J. Preskill, “Quantum computing in the NISQ era and beyond,” *Quantum*, vol. 2, p. 79, 2018.
- [17] J. R. McClean, S. Boixo, V. N. Smelyanskiy, R. Babbush, and H. Neven, “Barren plateaus in quantum neural network training landscapes,” *CoRR*, vol. abs/1803.11173, 2018.
- [18] J. Roffe, “Quantum error correction: an introductory guide,” *Contemporary Physics*, vol. 60, no. 3, p. 226–245, 2019.
- [19] Z. Cai, R. Babbush, S. C. Benjamin, S. Endo, W. J. Huggins, Y. Li, J. R. McClean, and T. E. O’Brien, “Quantum error mitigation,” *Reviews of Modern Physics*, vol. 95, no. 4, 2023.
- [20] T. Peng, A. W. Harrow, M. Ozols, and X. Wu, “Simulating large quantum circuits on a small quantum computer,” *Physical Review Letters*, 2020.
- [21] W. Tang, T. Tomesh, M. Suchara, J. Larson, and M. Martonosi, “Cutqc: using small quantum computers for large quantum circuit evaluations,” in *Proceedings of the 26th ACM International Conference on Architectural Support for Programming Languages and Operating Systems*, 2021.
- [22] A. Lowe *et al.*, “Fast quantum circuit cutting with randomized measurements,” *Quantum*, vol. 7, 2023.
- [23] C. Piveteau and D. Sutter, “Circuit knitting with classical communication,” *IEEE Transactions on Information Theory*, 2024.
- [24] G. Gentina, F. Metz, and G. Carleo, “Overhead-constrained circuit knitting for variational quantum dynamics,” *Quantum*, 2024.
- [25] M. Bechtold, J. Barzen, F. Leymann, A. Mandl, J. Obst, F. Truger, and B. Weder, “Investigating the effect of circuit cutting in qaoa for the maxcut problem on nisq devices,” *Quantum Science and Technology*, 2023.
- [26] S. Brandhofer, I. Polian, and K. Krsulich, “Optimal partitioning of quantum circuits using gate cuts and wire cuts,” *IEEE Transactions on Quantum Engineering*, vol. 5, pp. 1–10, 2024.
- [27] L. Schmitt, C. Piveteau, and D. Sutter, “Cutting circuits with multiple two-qubit unitaries,” *CoRR*, vol. abs/2312.11638, 2024.
- [28] A. W. Harrow and A. Lowe, “Optimal quantum circuit cuts with application to clustered hamiltonian simulation,” *CoRR*, vol. abs/2403.01018, 2024.
- [29] M. Bechtold, J. Barzen, F. Leymann, and A. Mandl, “Cutting a wire with non-maximally entangled states,” in *2024 IEEE International Parallel and Distributed Processing Symposium Workshops (IPDPSW)*, 2024.
- [30] D. T. S. Chen, Z. H. Saleem, and M. A. Perlin, “Quantum circuit cutting for classical shadows,” *ACM Transactions on Quantum Computing*, vol. 5, no. 2, p. 1–21, 2024.
- [31] S. Kan *et al.*, “Scalable circuit cutting and scheduling in a resource-constrained and distributed quantum system,” *CoRR*, vol. abs/2405.04514, 2024.
- [32] S. Sarker *et al.*, “Quantifying performance of wire-based quantum circuit cutting with entanglements,” in *2024 IEEE International Parallel and Distributed Processing Symposium Workshops (IPDPSW)*, 2024.
- [33] E. Pednault, “An alternative approach to optimal wire cutting without ancilla qubits,” *CoRR*, vol. abs/2303.08287, 2023.
- [34] H. Harada, K. Wada, and N. Yamamoto, “Doubly optimal parallel wire cutting without ancilla qubits,” *CoRR*, vol. abs/2303.07340, 2023.
- [35] E. Alpaydin and F. Alimoglu, “Pen-Based Recognition of Handwritten Digits,” *UCI Machine Learning Repository*, 1998.
- [36] D. Arthur and P. Date, “Hybrid quantum-classical neural networks,” in *IEEE International Conference on Quantum Computing and Engineering (QCE)*, pp. 49–55, IEEE, 2022.
- [37] S. Bhowmik and H. Thapliyal, “Transfer learning based hybrid quantum neural network model for surface anomaly detection,” *CoRR*, vol. abs/2409.00228, 2024.
- [38] R. Wang, F. Baba-Yara, and F. Chen, “Justq: Automated deployment of fair and accurate quantum neural networks,” in *ASP-DAC*, 2024.
- [39] M. A. Hafeez, A. Munir, and H. Ullah, “H-qnn: A hybrid quantum-classical neural network for improved binary image classification,” *AI*, 2024.
- [40] A. Senokosov, A. Sedykh, A. Sagingalieva, B. Kyriacou, and A. Melnikov, “Quantum machine learning for image classification,” *Mach. Learn. Sci. Technol.*, vol. 5, no. 1, p. 15040, 2024.
- [41] K. Zaman, T. Ahmed, M. Kashif, M. A. Hanif, A. Marchisio, and M. Shafique, “Studying the impact of quantum-specific hyperparameters on hybrid quantum-classical neural networks,” *CoRR*, vol. abs/2402.10605, 2024.
- [42] N. Schillo and A. Sturm, “Quantum circuit learning on nisq hardware,” *CoRR*, vol. abs/2405.02069, 2024.
- [43] K. Beer, D. Bondarenko, T. Farrelly, T. Osborne, R. Salzmann, D. Scheiermann, and R. Wolf, “Training deep quantum neural networks,” *Nature Communications*, vol. 11, p. 808, 2020.
- [44] P. Li, J. Liu, H. P. Patil, P. Hovland, and H. Zhou, “Enhancing virtual distillation with circuit cutting for quantum error mitigation,” in *2023 IEEE 41st International Conference on Computer Design (ICCD)*, 2023.
- [45] R. Majumdar and C. J. Wood, “Error mitigated quantum circuit cutting,” *CoRR*, vol. abs/2211.13431, 2022.
- [46] S. Basu *et al.*, “Fragqc: An efficient quantum error reduction technique using quantum circuit fragmentation,” *Journal of Systems and Software*, 2024.
- [47] S. C. Marshall, C. Gyurik, and V. Dunjko, “High dimensional quantum machine learning with small quantum computers,” *Quantum*, 2023.
- [48] S. Bilek, “Utilizing small quantum computers for machine learning and ground state energy approximation,” *CoRR*, vol. abs/2403.14406, 2024.
- [49] Y. Kawase, “Distributed quantum neural networks via partitioned features encoding,” *Quantum Machine Intelligence*, 2024.
- [50] N. Innan, M. A.-Z. Khan, A. Marchisio, M. Shafique, and M. Bennai, “Fedqnn: Federated learning using quantum neural networks,” 2024.
- [51] L. Deng, “The mnist database of handwritten digit images for machine learning research [best of the web],” *IEEE Signal Processing Magazine*, 2012.
- [52] C.-C. Chen, M. Watabe, K. Shiba, M. Sogabe, K. Sakamoto, and T. Sogabe, “On the expressibility and overfitting of quantum circuit learning,” *ACM Transactions on Quantum Computing*, 2021.
- [53] M. Kobayashi, K. Nakaji, and N. Yamamoto, “Overfitting in quantum machine learning and entangling dropout,” *Quantum Mach. Intell.*, 2022.
- [54] F. Scala, A. Ceschini, M. Panella, and D. Gerace, “A General Approach to Dropout in Quantum Neural Networks,” *Adv. Quantum Technol.*, 2023.
- [55] A. R. Shinde, C. Jain, and A. Kalev, “A post-training approach for mitigating overfitting in quantum convolutional neural networks,” *CoRR*, vol. abs/2309.01829, 2024.